ACS SENSORS

Article

Cite This: ACS Sens. 2019, 4, 1417−1423

pubs.acs.org/acssensors

Directly Accessible and Transferrable Nanofluidic Systems for Biomolecule Manipulation

Yun-Soung Kim,[†] Brian M. Dincau,[‡] Young-Tae Kwon,[†] Jong-Hoon Kim,*[,‡] and Woon-Hong Yeo*[,†,§]

[†]George W. Woodruff School of Mechanical Engineering, Institute for Electronics and Nanotechnology and [§]Wallace H. Coulter Department of Biomedical Engineering, Parker H. Petit Institute for Bioengineering and Biosciences, Center for Flexible and Wearable Electronics Advanced Research, Institute for Materials, Georgia Institute of Technology, Atlanta, Georgia 30332, United States

[‡]School of Engineering and Computer Science, Washington State University, Vancouver, Washington 98686, United States

Supporting Information

ABSTRACT: Molecular detection and manipulation via nanofluidic systems offers new routes for single-molecule analysis to study epigenetic mechanisms and genetic mutation of disease. For detection of single biological molecule, many types of nanomicrofluidic systems have been utilized. Typically, mechanical tethering, fluidic pressure, chemical interactions, or electrical forces allow controllable attraction, enrichment, confinement, and elongation of target molecules. The currently available methods, however, are unable to offer both molecular manipulation and direct and concurrent assessment of target molecules in the system due to the nature of enclosed channels and associated fluidic components. Here, we introduce a wafer-scale nanofluidic system that incorporates an array of accessible open nanochannels and nano-microtrappers to enrich and elongate target molecules (DNA) via the combination of an electric field and hydrodynamic force. The open nanofluidic system allows easy access, direct observation, and manipulation of molecules in the nanochannels. The presence of a stretched single DNA and the efficacy of the nanofluidic system are studied by fluorescence microscopy and atomic force microscopy. Hybrid integration of the nanodevice fabrication with a material transfer printing technique enables to design a highly flexible and transferrable nanofluidic system after molecular concentration.

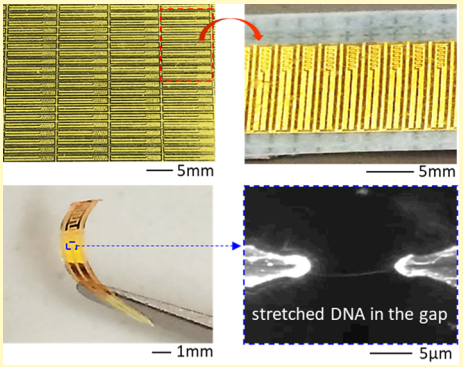

KEYWORDS: *nanofluidic system, wafer-scale fabrication, direct assessment of molecules, nanochannels, and flexible and transferrable nanosystem*

The study of the single molecule and detection of its dynamic change is one of the major topics in genome research and disease mutation.[1,2] To fully understand the biological processes, it is critical to directly observe biochemical interactions on or near an individual DNA strand. Biomolecules, such as DNA polymerase and small interfering RNA (siRNA), interact with DNA to facilitate replication, transcription, and gene silencing or activation. However, the study of these molecular interactions can be limited in optical microscopic observation if the DNA strand is directly inaccessible via physical bindings. A direct contact capability to stretched DNA could open up many opportunities to further analyze the DNA with different dye intercalation, oligomer hybridization, and protein binding. Thus, single molecule analysis is necessary[3] to investigate interactions with regulatory molecules and to determine the specific ordering and orientation of markers associated with various disease states at epigenetic levels. Recent years have witnessed rapid progress in developing approaches[4−8] for single molecule extension, such as DNA stretching using optical tweezers, magnetic tweezers, microfluidic channels, paired interdigitated electrodes, and nanofluidic confinement. While all of these techniques enable single-molecule experiments, most of them also require a repetition of difficult or tedious procedure to obtain statistically meaningful results. Among these methods, confinement-based molecular stretching[9−12] has attracted great interest, due to its simple mechanism and potential for parallelization. Since DNA can be elongated by reducing the dimensions of the nanoscale confinement, nanochannels with widths slightly larger than the diameter of double helical DNA molecules could drive the extension of DNA molecules to their full contour lengths. For example, DNA barcoding system[13] has been exploited, enabling a direct approach for acquisition of genome sequence information. However, the fabrication of the small nanochannels with long lengths is extremely challenging since the formation of such nanostructures generally requires advanced and cost-prohibitive nanofabrication technologies. Technical hurdles, such as the reduced DNA loading efficiency and the limitation in direct assessment of the

Received: March 7, 2019
Accepted: May 7, 2019
Published: May 7, 2019

DOI: 10.1021/acssensors.9b00470
ACS Sens. 2019, 4, 1417−1423

confined molecules for post-manipulation in genomic sequencing and mapping, prevent the technology to be widely adopted.

Here, we report a high-throughput, high-yield nanofluidic system that enables effective concentration and detection of stretched DNA in nanochannels, integrated with trapping electrodes. Due to its polarizability, DNA can be translocated using an inhomogeneous electric field, otherwise known as dielectrophoresis (DEP). DEP offers great advantages for controlled manipulation of DNA molecules as it is noninvasive, nondestructive, and fast. DEP relies solely on the dielectric properties of the target particle; thus, it is inherently selective.[14,15] In this system, DEP force is used to attract DNA between paired microelectrodes and nanochannel confines the target for further stretching with easy accessibility in the open fluidic configuration. Therefore, the nanofluidic system employs the DEP force for the initial migration of DNA molecules, and open-channel fluidic confinement for the final alignment and immobilization. Stretched DNA that is stained by fluorescent particles in the nanochannels are directly observed through fluorescence microscopy and verified by atomic force microscopy (AFM). This system can incorporate hundreds of immobilization sites, significantly improving yield and reducing the requirement for repetitive sample preparation. Implementation of the wafer-scale, large array nanofluidic systems for molecular stretching has the potential to optically barcode target molecules at specific sequences and rapidly map the binding sites of interest back to the human genome, which can create a direct genome-wide mapping to study epigenetic modifications.

RESULTS AND DISCUSSION

For a wafer-scale fabrication of nanostructure channels, we utilized a shadow-enabled lithography method,[16] as depicted in Figure 1a (details of the process appear in Experimental Section). This technique uses the shadow effect in high-vacuum electron beam evaporation of a metal (Al) to make shadow nanogaps on a Si wafer. Uniform nanogaps were formed through a gap compensation method (two consecutive deposition of Al layers) on a 200-nm-thick silicon dioxide (SiO_2) layer, thermally grown on the Si wafer. Reactive ion etching followed to create nanochannels on the nanogaps where the channel depth was controlled by the etching rate and time. Figure 1b shows an example photo of a 4 inch Si wafer having an array of the fabricated nanochannels. Figure 1c,d presents some of the nanochannel array, imaged by scanning electron microscopy (SEM); the final dimension of the fabricated nanochannels is 50 nm in width, 100 nm in depth, and 10 μm in spacing. In this work, the manufactured nanochannels are used as an open fluidic system to deliver sample solutions that include biomolecules such as DNA.

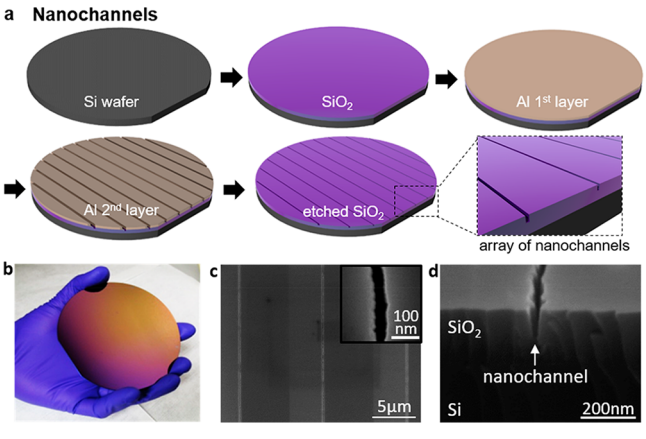

Figure 1. Fabrication strategy of a wafer-scale nanofluidic system, including an array of nanochannels. (a) Illustration of a step-by-step process of a nanochannel fabrication. (b) Photo of a Si wafer including an array of fabricated nanochannels. (c,d) SEM images of the fabricated nanochannel array where the inset in (c) shows a top-view of a single nanochannel, while (d) shows a cross-sectional view of the nanochannel in SiO_2.

In addition, we utilized another manufacturing approach that combines photolithographic patterned microtrappers with focused ion-beam patterned nanochannels, which developed a directly accessible nanofluidic system for biomolecules. Figure 2 summarizes the fabrication strategy of microscale trappers with nanochannels (referred to as "nano-microtrapper"). As for a low-cost, large-scale manufacturing, the nanochannel patterning might be replaced by the shadow-edge lithographic method.[16] Similar to the open nanochannels in Figure 1, we used a 4 in. SiO_2 deposited Si wafer as the base template to construct nano-microtrappers, which offer addressable, direct molecule detection and transfer for multistage molecular analysis. A typical microfabrication process designed the nanofluidic structure via metallization of Au deposition (30 nm) and photolithography (Figure 2a). An array of paired microtrappers having 10 μm gaps was patterned over the Si wafer, which was diced into individual chips (dimension: 1 × 10 mm^2) for molecular imaging and transfer (Figure 2b,c). Afterward, nanoscale channels were added on top of the microtrappers for stretching of attracted biomolecules to the trappers. Focused ion beam created such channel between a pair of microtrappers (Figure 2d).

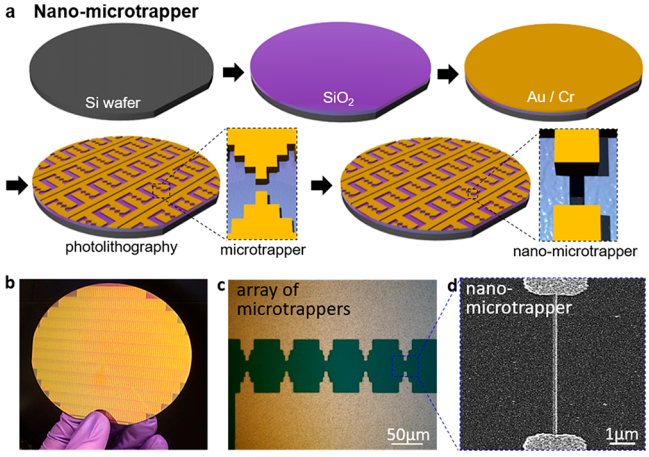

Figure 2. Fabrication strategy of an array of nano-microtrapper. (a) Illustration of a fabrication process for an array of nano-microtrappers on a Si wafer. (b) Photo of a Si wafer having an array of fabricated nano-microtrappers. (c) Optical microscope image showing a set of microtrappers. (d) SEM image of a nano-microtrapper created by a focused ion beam.

To study molecular insertion and stretching in nanochannels, we explored λ-DNA (New England Biolabs). The concentration of the initial DNA solution was 500 μg/mL in Tris-EDTA buffer (pH 7.5, Sigma-Aldrich). The final concentration of λ-DNA for the stretching experiment was prepared as 500 ng/mL through multiple dilutions with the

DOI: 10.1021/acssensors.9b00470
ACS Sens. 2019, 4, 1417−1423

buffer solution. An intercalating dye (PicoGreen, Invitrogen) was used to stain the target DNA for direct observation of molecular introduction into the channels via fluorescence microscopy (Nikon Eclipse). An experimental setup in this study (Figure 3a) includes a wafer with an array of the

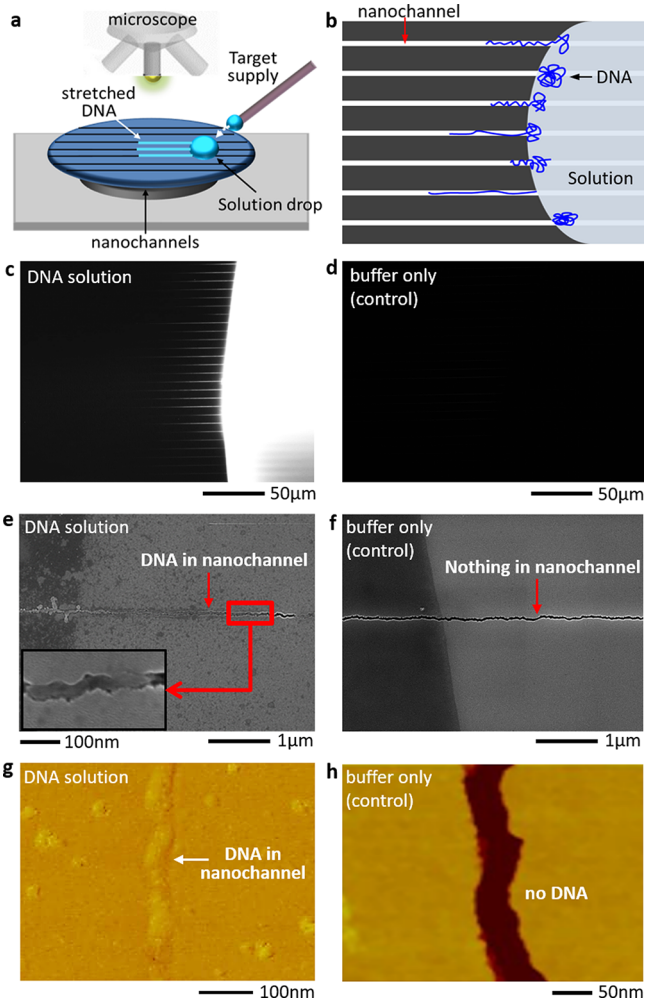

Figure 3. Molecular detection with nanochannels. (a) Experimental setup that includes an array of nanochannels, fluorescence microscope, and a syringe pump. (b) DNA molecules in the buffer solution are inserted and stretched through the nanochannels due to the diffusion of cations in the solution. (c,d) Fluorescence microscope images of showing stretched DNA molecules in the nanochannels (c) and a control result with a buffer solution only (d). (e,f) SEM images that capture DNA in a nanochannel (e) and control (f). (g,h) AFM images that are corresponding to the SEM images (e,f).

fabricated nanochannels (Figure 1), a fluorescence microscope with a cooled CCD camera and a syringe pump (Harvard Apparatus) to deliver the DNA solution to the nanochannels. As a substrate, SiO_2 is ideal to create uniform nanochannels due to the smooth surface, while Al is an ideal patterning metal since a highly controllable, uniform film can be made in electron beam evaporation. DNA molecules in the buffer solution were inserted and stretched through the nanochannels (Figure 3b) due to the diffusion of cations in the solution.[17] The 50-nm-wide channels allowed a full DNA stretching by considering the persistence length of DNA in a buffer solution (about 40 nm).[18] It should be noted that 10 μm spacing was the limitation of the shadow-enabled lithography method,[16] caused by the minimum feature size (~5 μm) of the conventional UV photolithography; since we used the shadow of the predefined feature, the minimum spacing became 10 μm. Ion diffusion into a nanochannel makes DNA inserted into the channel and stretched sequentially (Figure 3b). The stretched DNA is directly observed by fluorescence microscopy (Figure 3c). As a negative control test, we used the buffer solution without DNA, mixed with the intercalating dye. The fluorescence microscope image in Figure 3d clearly shows no signals from the channels, compared to the image in Figure 3c. In addition, we further investigated the captured DNA in nanochannels via SEM and AFM studies. As summarized in Figure 3e and f, the stretched DNA in Figure 3c could be directly delivered for SEM investigation, which clearly shows the presence of DNA molecules in the nanochannel. Similarly, the open nanochannel configuration allows a direct observation of the DNA via AFM study (Figure 3g and h). Overall, this study captures the major advantage of the directly and easily accessible nanofluidic system for molecular detection (λ-DNA in this case) without detaching the channel enclosure and other solution delivery components that are normally used in the existing systems.[17,19,20]

In addition, we explored another nanofluidic platform, named a nano-microtrapper, to directly investigate biomolecules (Figure 4). An experimental setup in Figure 4a includes an individual electrode chip with an array of nano-microtrappers, a solution chamber that includes 5 μL sample solution, and a signal generator for an AC electric field. The electrode chip was precoated with poly(L-lysine) (PLL, Sigma-Aldrich) to ensure a uniform surface condition; the uniform wettability was important to maintain smooth movement of solution meniscus upon the withdrawal of the chip (Figure 4b) from the solution drop (Figure 4c). Without this coating, the meniscus is disturbed by the alternating SiO_2 and Au layers. The display shows an electrode-chip immersed in the solution. Due to capillary action, the semicircular meniscus was generated on the chip surface. In addition, the enriched molecules could be immobilized on the chip surface due to an electrostatic force between positively charged PLL and negatively charged molecule such as DNA. To attract and concentrate the target molecules (λ-DNA), we utilized DEP based on the applied AC field. It should be noted that the open nanofluidic system, presented here, may include a solution evaporation. However, for the case of nanochannels, the evaporation of a solution drop was associated with a coffee ring effect,[21] which helped to concentrate DNA at the edge of the drop for expedited insertion into the nanochannels. For the case of nano-microtrappers, the chip was actively controlled to pull out of a solution with the withdrawal speed of 50 μm/s. The control speed was fast enough that no adverse effect from evaporation was observed in DNA capture. Therefore, our work shows negligible drawbacks from the solution evaporation. Our future work will focus on a controlled, quantitative study to further investigate the evaporation effect on the change of capillary action. When a PLL-treated electrode-chip was immersed into a solution drop, molecules such as DNA were polarized and attracted to the tip of microelectrodes where the highest electric field gradient occurred. The attracted DNA was anchored at one electrode tip by DEP and stretched by capillary forces at the meniscus when the electrode-chip was withdrawn from the solution drop. The withdrawal speed was 50 μm/s, which was chosen not to sweep DNA away from the electrode. The AC field was

DOI: 10.1021/acssensors.9b00470
ACS Sens. 2019, 4, 1417−1423

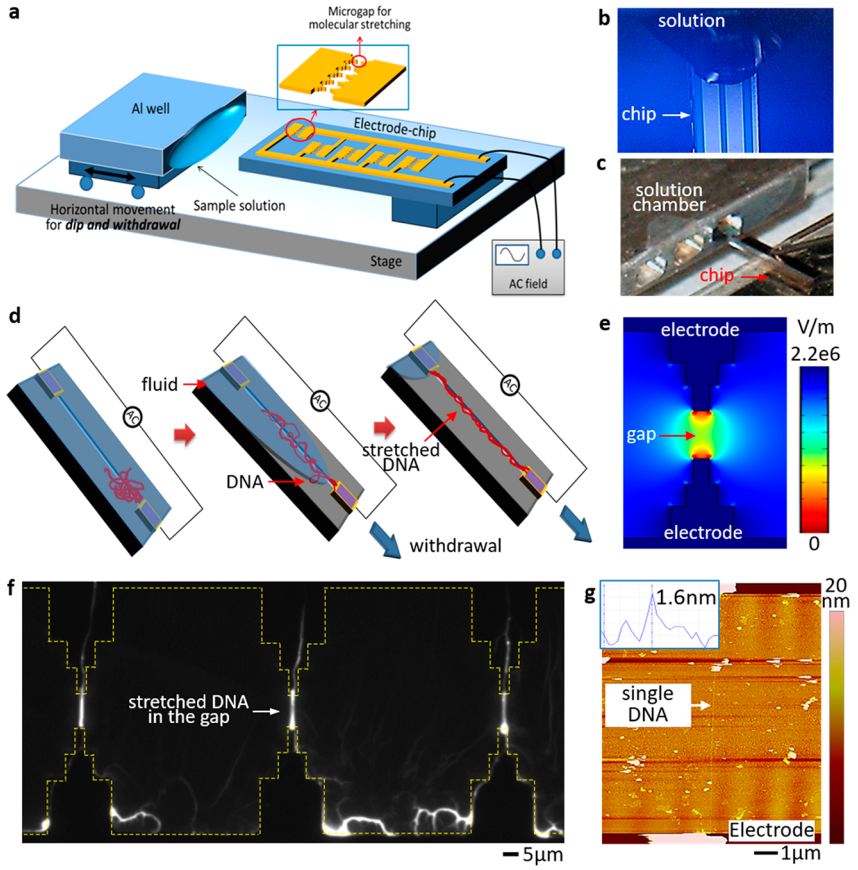

Figure 4. Direct molecular enrichment and detection via nano-microtrappers. (a) Experimental setup, including an individual electrode chip, solution chamber, control stage, and signal generator. (b,c) Photos of showing a chip withdrawal (b) from the solution drop in the Al chamber (c). (d) Illustration that describes a sequential process of DNA anchoring to the electrode by DEP and follow-up stretching by capillary action. (e) Computational calculation of the electric field strength, showing the highest values at the terminal ends of the electrodes. (f) Fluorescence microscope image of the stretched DNA molecules in the electrode gaps with the yield of 90% (18 out of 20 pairs of electrodes). (g) Atomic force microscopy that captures the presence of a stretched single DNA molecule between a pair of electrodes. Inset graph shows the height of the single DNA.

continuously supplied until the chip was fully withdrawn. As shown in Figure 3c, lengths of stretched DNA vary per channel, which can be explained by nonuniform ion diffusion. When a DNA solution is dropped on the array of nanochannels, cations in the DNA solution form the electrical double layer on the surface of the SiO_2 layer. Through the diffusion of cations, the DNA molecules are introduced and stretched in the confined nanochannels. Thus, the stretched length is dependent on the ion concentration per each channel. Due to time and temperature-dependent diffusion, the ion concentration in a solution drop is not uniform, which may result in nonuniform stretching of DNA. Since the utilized λ-DNA was stained with an intercalating dye, the stretched DNA could be immediately observed by fluorescence microscopy. Figure 4d illustrates the underlying mechanism of DEP to enrich DNA molecules to the gap between the nano-microtrapper, which is stretched by the fluid flow. The DNA molecule is initially anchored to the terminal end of an electrode (Figure 4d) due to the highest electric field strength, validated by the computational modeling in Figure 4e (COMSOL Multiphysics). The stretched DNA molecules in an array of nano-microtrappers are shown in Figure 4f, captured by fluorescence microscopy. The fluorescence microscopy observation shows that DNA was successfully immobilized and elongated on multiple nano-microtrappers (details in Figure S1). As a negative control, we tested two cases where no electric field was used during the capture and no DNA was present in the solution. No fluorescence signals were observed in these cases (Figure S2). Subsequently, atomic force microscopy verified the presence of a stretched single DNA molecule between a pair of electrodes (Figure 4g). We used a tapping mode to gently detect the soft DNA on the chip (details of the atomic force microscopy investigation appear in the Experimental Section). In the image, the white dots are ionic crystals that are present in the DNA buffer solution. The measured height of the stretched DNA was ~1.6 nm, which demonstrated a single DNA molecule. The stretched length of λ-DNA was 10.5 μm, which was the same as the gap size between two microelectrodes. Collectively, the molecular trapping and stretching study with the nano-microtrappers captures the potential of the newly developed nanofluidic system for high-throughput assembly of DNA molecules. In comparison with the aforementioned nanochannel system, the nano-microtrapper system provides a full access to the captured molecules and easy transfer and storage opportunities for extensive post-analysis. On the other hand, the nano-channels have advantages in easier and simpler fabrication than the nano-microtrappers, while offering fast capture and stretching of target molecules.

DOI: 10.1021/acssensors.9b00470
ACS Sens. 2019, 4, 1417−1423

Even though molecular detection in epigenetics and disease diagnostics requires extensive post-analysis, the existing nanofluidic systems are still limited in the device portability and possible transfer for follow-up study in various methods. In this work, we developed a new fabrication method, combining the conventional microfabrication[12,22] and material transfer printing, for a flexible microchip that can be transferrable (Figure 5). We utilized a flexible polymer membrane

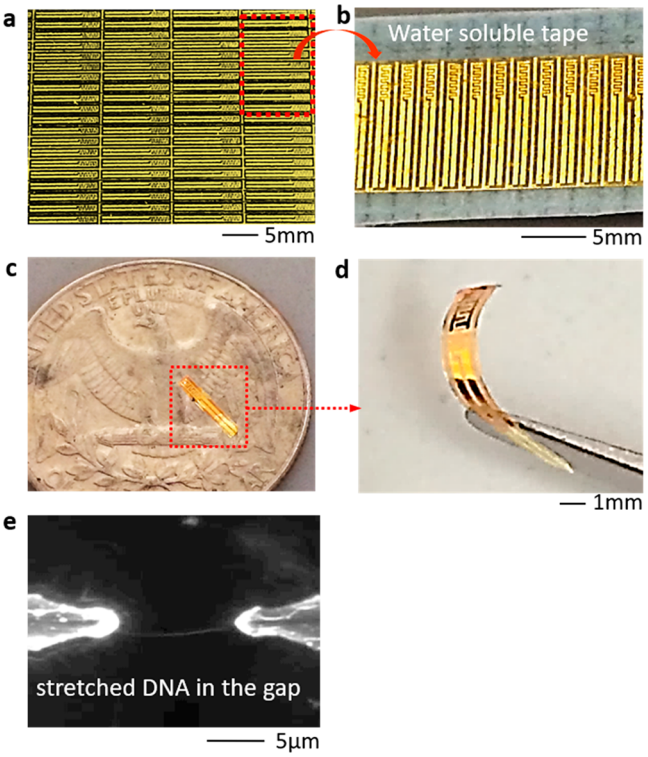

Figure 5. Flexible and transferrable nanofluidic system. (a) Photo of an array of flexible nano-microtrappers on a PDMS membrane. (b) Detached nano-microtrappers from the carrying substrate, facilitated by heating the substrate. (c) Photo of a flexible single chip on a quarter dollar, after dissolving the water-soluble tape. (d) Magnified view of the chip. (e) Fluorescence microscope image showing the captured and stretched DNA in the electrode gap.

(polyimide; PI with 1 μm in thickness, HD MicroSystems) and an elastomeric membrane (polydimethylsiloxane; PDMS). A PI layer was spin-coated and cured on a PDMS-deposited Si wafer. Afterward, metallization and photolithography was used to define the microtrapper structure (details of the fabrication process appear in the Experimental Section and Figure S3). A thin Cr layer was not needed in this case since Au had a great adhesion to the PI substrate. A photo in Figure 5a captures a part of the fabricated device, showing an array of flexible microtrappers, which can be easily dissociated from the carrying wafer by a water-soluble tape. Heating of the PDMS substrate on a hot plate (100 °C) could facilitate the releasing process. The retrieved chips (Figure 5b) were used to capture and stretch DNA molecules by following the same procedure, described in Figure 4. A representative example in Figure 5c,d shows a flexible chip after the DNA manipulation and corresponding fluorescence image that captures a DNA molecule. The individual chip with DNA can be easily delivered to other locations for necessary post-analysis, while enabling a long-term storage of the entire device. These chips are well suited for automatic processing, given their tight, ordered clustering, integrated electrodes, and predefined periodic analysis locations.

CONCLUSION

We have demonstrated the feasibility of a wafer-scale fabrication method to design a directly accessible nanofluidic system. The open nanofluidic devices enable timely observation of captured biomolecules via different types of microscopic analysis, without the need of dissociation of other fluidic components. An array of nanochannels and nano-microtrappers successfully capture targeted DNA molecules from a sample solution, which are clearly detected by fluorescence and atomic force microscopy. Integration of a newly developed transfer printing technique to the microfabrication allows the design of a flexible and transferrable device that can find various applications in consecutive molecular analysis, device transfer, and long-term storage.

EXPERIMENTAL SECTION

Preparation of λ-DNA. λ-DNA (48.5 kbp, New England BioLabs) was purchased for the study of molecular stretching. The concentration of the initial DNA solution was 500 μg/mL (16 nM, molecular weight: 31.5 × 10^6 Da) in TRIS EDTA (TE) buffer (pH 7.5). The final concentration of λ-DNA for the stretching experiment was 500 ng/mL, which was diluted from the original solution by 1000-fold. To detect DNA molecules, an intercalating dye (PicoGreen, Invitrogen) was used, which was green fluorophoric dye. Following the protocol of the kit, PicoGreen solution was diluted by 200-fold with 1 × TE buffer. Prior to the DNA experiment, λ-DNA solution was mixed with the diluted PicoGreen with the volume ratio of 1:1. To observe the stretched DNA molecules, a fluorescence microscope (Nikon Eclipse) was used with a CCD camera and imaging software.

Experimental Setup. The experimental setup for λ-DNA stretching includes a probe station to place a control stage and probes for electrical connection. The *xyz* stage was used to control of Al well movement (Figure 4). To apply an ac electric field, a function generator (Agilent 33220A, Santa Clara, CA) was used. The electric potentials were 20 V_{pp} at 5 MHz for λ-DNA stretching. The experiment process was monitored by an optical microscope. The electrode-chip having a microelectrode array was placed on the stage with Al well, which could hold a 5 μL sample solution. In addition, poly(L-lysine) (PLL) solution (0.1% w/v in water; P8920, Sigma-Aldrich) was diluted by 100-fold with pure water. The diluted solution was used to coat the surface of an electrode-chip.

Nano-Microtrapper. The microtrapper was fabricated out of gold on a 4 in silicon wafer. The wafer was first oxidized to create an insulating barrier. 10 nm of chromium was sputtered onto the 300-nm-thick oxide layer to serve as an adhesion layer, followed by 20 nm of sputtered gold. The microtrapper geometries were patterned through standard photolithography with a positive-tone photoresist (AZ1518, MicroChemicals). The exposed metal layers were then etched using wet chemicals (Transene Gold Etch type TFA and Transene Chromium Etchant 1020). The remaining photoresist was stripped in an acetone bath, and then a thin sacrificial layer of photoresist was applied prior to dicing in order to protect the soft gold features. After dicing, the microtrappers were cleaned with acetone, isopropyl alcohol, and deionized (DI) water. The individual chip was then mounted on a stub using carbon tape and inserted into the focused ion beam (FIB) instrument (FEI Quanta 3D 200i, dual beam system) with a 30 kV Ga+ beam extracted from a liquid metal ion source. The milled nanochannel layout is shown in Figure 2d.

Experimental Procedure for λ-DNA Stretching with Nano-Microtrapper. The experimental procedure for molecular stretching is as follows: (1) Blow an electrode-chip surface a few times with a nitrogen gun to remove particles. (2) Drop 2 μL of the diluted PLL

DOI: 10.1021/acssensors.9b00470
ACS Sens. 2019, 4, 1417−1423

solution on the electrode-chip, and wait for 1 min. (3) Rinse the chip in pure water 3 times and dry the chip with a nitrogen gun. (4) Install the PLL-coated chip and Al well on the *xyz* stage. (5) Drop 5 μL of λ-DNA solution in the well. (6) Apply an ac electric field on the electrode-chip, and dip into the solution drop. (7) After 3 min, the electrode-chip was withdrawn from the solution through the horizontal motion of the Al well. (8) Transfer the electrode-chip to a fluorescence microscope and an atomic force microscope for detection of molecules.

Flexible Microtrapper. The flexible electrodes were fabricated in a similar manner to the rigid electrodes, with the inclusion of a flexible substrate layer. To act as a release layer, a thin sheet of polydimethylsiloxane (PDMS) was applied to a silicon wafer via spin coating at 3000 rpm for 1 min. The PDMS was mixed in a 10:1 ratio prior to spin coating, then baked on a hot-plate at 150 °C for 30 min to rapidly cure after application. The PDMS-coated wafer was treated with ultraviolet (UV) by using a UV lamp (8.9 mW/cm^2) for 3 min to make the surface hydrophilic. A thin layer (<5 μm) of polyimide (PI) was then spun on top of the PDMS layer at 4000 rpm for 1 min and baked on a hot plate at 150 °C for 5 min to serve as the flexible substrate for the final electrode. Through sputter deposition, a 100 nm gold layer was applied to the PI layer, followed by the same patterning and etching steps as the rigid electrode.

■ ASSOCIATED CONTENT

Supporting Information

The Supporting Information is available free of charge on the ACS Publications website at DOI: 10.1021/acssensors.9b00470.

> Yield of the captured DNA on nano-microtrappers. Fluorescence images of the negative control experimental results. Fabrication process of the transferrable nanofluidic system. (PDF)

■ AUTHOR INFORMATION

Corresponding Authors

*E-mail: whyeo@gatech.edu.
*E-mail: jh.kim@wsu.edu.

ORCID

Woon-Hong Yeo: 0000-0002-5526-3882

Author Contributions

Y.K., B.D., J.-H.K., and W.-H.Y. conceived and designed the research; Y.K., B.D., Y.-T.K., J.-H.K., and W.-H.Y. performed the experiment and analyzed the data; Y.K., B.D., J.-H.K., and W.-H.Y. wrote the paper.

Notes

The authors declare no competing financial interest.

■ ACKNOWLEDGMENTS

W.-H.Y. acknowledges a grant from the Samsung Global Technology Center. This research was supported in part by funds from the Marcus Foundation, The Georgia Research Alliance, and the Georgia Tech Foundation through their support of the Marcus Center for Therapeutic Cell Characterization and Manufacturing (MC3M) at Georgia Tech. This work was performed in part at the Institute for Electronics and Nanotechnology, a member of the National Nanotechnology Coordinated Infrastructure, which is supported by the National Science Foundation (Grant ECCS-1542174). J.-H. K. acknowledge partial financial support from the Washington State University New Faculty Seed Grant (131078) and the National Science Foundation (NSF CBET- 1707056).

■ REFERENCES

(1) Restrepo-Pérez, L.; Joo, C.; Dekker, C. Paving the way to single-molecule protein sequencing. *Nat. Nanotechnol.* **2018**, *13* (9), 786–796.

(2) Ardui, S.; Ameur, A.; Vermeesch, J. R.; Hestand, M. S. Single molecule real-time (SMRT) sequencing comes of age: applications and utilities for medical diagnostics. *Nucleic Acids Res.* **2018**, *46* (5), 2159–2168.

(3) Yu, M.; Hou, Y.; Song, R.; Xu, X.; Yao, S. Tunable Confinement for Bridging Single-Cell Manipulation and Single-Molecule DNA Linearization. *Small* **2018**, *14* (17), 1800229.

(4) Schakenraad, K.; Biebricher, A. S.; Sebregts, M.; Ten Bensel, B.; Peterman, E. J. G.; Wuite, G. J. L.; Heller, I.; Storm, C.; van der Schoot, P. Hyperstretching DNA. *Nat. Commun.* **2017**, *8* (1), 2197.

(5) Dulin, D.; Cui, T. J.; Cnossen, J.; Docter, M. W.; Lipfert, J.; Dekker, N. H. High Spatiotemporal-Resolution Magnetic Tweezers: Calibration and Applications for DNA Dynamics. *Biophys. J.* **2015**, *109* (10), 2113–2125.

(6) Dorfman, K. D.; King, S. B.; Olson, D. W.; Thomas, J. D.; Tree, D. R. Beyond gel electrophoresis: microfluidic separations, fluorescence burst analysis, and DNA stretching. *Chem. Rev.* **2013**, *113* (4), 2584–2667.

(7) Holzel, R.; Gajovic-Eichelmann, N.; Bier, F. F. Oriented and vectorial immobilization of linear M13 dsDNA between interdigitated electrodes - towards single molecule DNA nanostructures. *Biosens. Bioelectron.* **2003**, *18* (5–6), 555–564.

(8) Yeh, J. W.; Taoni, A.; Chen, Y. L.; Chou, C. F. Entropy-Driven Single Molecule Tug-of-War of DNA at Micro-Nanofluidic Interfaces. *Nano Lett.* **2012**, *12* (3), 1597–1602.

(9) Schakenraad, K.; Biebricher, A. S.; Sebregts, M.; ten Bensel, B.; Peterman, E. J.; Wuite, G. J.; Storm, C.; van der Schoot, P.; Heller, I. Hyperstretching DNA. *Biophys. J.* **2018**, *114* (3), 90a.

(10) Jiang, K.; Humbert, N.; Kalyanavenkatramanan, S. K.; Mely, Y.; Westerlund, F. Interactions between DNA and HIV-1 Nucleocapsid Protein Studied using Nanofluidic Channels. *Biophys. J.* **2018**, *114* (3), 89a–90a.

(11) Westerlund, F.; Persson, F.; Fritzsche, J.; Beech, J. P.; Tegenfeldt, J. O. Fluorescence Microscopy of Nanochannel-Confined DNA. *Single Molecule Analysis*; Springer: 2018; pp 173–198.

(12) Dincau, B. M.; Lee, Y.; Kim, J.-H.; Yeo, W.-H. Recent advances in nanoparticle concentration and their application in viral detection using integrated sensors. *Sensors* **2017**, *17* (10), 2316.

(13) Jo, K.; Dhingra, D. M.; Odijk, T.; de Pablo, J. J.; Graham, M. D.; Runnheim, R.; Forrest, D.; Schwartz, D. C. A single-molecule barcoding system using nanoslits for DNA analysis. *Proc. Natl. Acad. Sci. U. S. A.* **2007**, *104* (8), 2673–2678.

(14) Viefhues, M.; Eichhorn, R. DNA dielectrophoresis: Theory and applications a review. *Electrophoresis* **2017**, *38* (11), 1483–1506.

(15) Yeo, W.-H.; Lee, H.-B.; Kim, J.-H.; Lee, K.-H.; Chung, J.-H. Nanotip analysis for dielectrophoretic concentration of nanosized viral particles. *Nanotechnology* **2013**, *24* (18), 185502.

(16) Bai, J. G.; Chang, C.-L.; Chung, J.-H.; Lee, K.-H. Shadow edge lithography for nanoscale patterning and manufacturing. *Nanotechnology* **2007**, *18* (40), 405307.

(17) Zhou, J.; Wang, Y.; Menard, L. D.; Panyukov, S.; Rubinstein, M.; Ramsey, J. M. Enhanced nanochannel translocation and localization of genomic DNA molecules using three-dimensional nanofunnels. *Nat. Commun.* **2017**, *8* (1), 807.

(18) Rocha, J.; Silva, E.; Oliveira, M.; Sousa, F.; Teixeira, A.; Rocha, M. β-Cyclodextrin polymer binding to DNA: Modulating the physicochemical parameters. *Phys. Rev. E: Stat. Phys., Plasmas, Fluids, Relat. Interdiscip. Top.* **2017**, *95* (5), No. 052416.

(19) Amin, S.; Khorshid, A.; Zeng, L.; Zimny, P.; Reisner, W. A nanofluidic knot factory based on compression of single DNA in nanochannels. *Nat. Commun.* **2018**, *9* (1), 1506.

(20) Sun, X.; Yasui, T.; Yanagida, T.; Kaji, N.; Rahong, S.; Kanai, M.; Nagashima, K.; Kawai, T.; Baba, Y. Nanostructures Integrated with a Nanochannel for Slowing Down DNA Translocation Velocity for Nanopore Sequencing. *Anal. Sci.* **2017**, *33* (6), 735–738.

DOI: 10.1021/acssensors.9b00470
ACS Sens. 2019, 4, 1417–1423

(21) Anyfantakis, M.; Baigl, D. Manipulating the Coffee-Ring Effect: Interactions at Work. *ChemPhysChem* **2015**, *16* (13), 2726−2734.
(22) Chen, Y.; Howe, C.; Lee, Y.; Cheon, S.; Yeo, W.-H.; Chun, Y. Microstructured thin film nitinol for a neurovascular flow-diverter. *Sci. Rep.* **2016**, *6*, 23698.

DOI: 10.1021/acssensors.9b00470
ACS Sens. 2019, 4, 1417−1423